Molecular Logic

DOI: 10.1002/anie.201000840

Colorimetric Logic Gates Based on Supramolecular DNAzyme Structures**

*Sai Bi, Yameng Yan, Shuangyuan Hao, and Shusheng Zhang**

An electronic integrated circuit system is composed of elementary logic gates, which are capable of performing Boolean logic by receiving Boolean inputs representing true (1, high voltage) or false (0, low voltage) values and generating the appropriate Boolean output.[1] Analogously, molecular computation, a term that includes a number of distinct bottom-up approaches toward the design of molecular-scale electronics, that is, chemical and biological computers, has become an alternative approach to computing technologies.[2] In recent decades, considerable efforts have been dedicated to problems in Boolean logic at the molecular scale in order to identify ideal candidates that satisfy logic operations. To this end, a variety of molecular Boolean logic gates based on supramolecular complexes and small molecules, enzymatic biochemical networks, biopolymer-ligand, and photonic interactions, and other systems have been devised.[3] However, most of these logic gates function by fluorescence detection, which often suffers from complex handling procedures and a lack of portability. In an alternative approach, homogeneous colorimetric detection methods based on the high extinction coefficients and strongly distance-dependent optical properties of Au nanoparticles (AuNPs) have become more and more attractive. These methods may minimize or even eliminate complex analysis procedures that involve expensive instrumentation, and hold great promise for low-cost, low-volume, and rapid readout of the analyte, and more convenient management for on-site detection.[4]

Metal ions play an important role for the environment and human health. For example, the Pb^{2+} ion is a common environmental pollutant that can lead to a number of adverse health effects at low-level exposure, especially in children.[5] Mg^{2+} ions act as an enzyme activator and are essential for neuromuscular excitability and cell permeability, and Mg^{2+} ion deficiency may increase the risk of artery spasm. The presence of Mg^{2+} ions in drinking water can be critical for Mg^{2+} ion content in the body.[6] Thus, rapid and sensitive monitoring methods for different ions in water or food resources are of great importance.

In recent years, DNAzymes have become attractive molecules for metal-ion sensing based on metal-dependent activities of specific DNAzymes, which can be easily isolated by systematic evolution of ligands by exponential enrichment (SELEX) or in vitro selection.[7] So far, DNAzymes that are specific for various metal ions such as Pb^{2+},[8] Mg^{2+},[9] UO_2^{2+}[10], and Cu^{2+}[11] have been obtained. The cofactor-dependent activity of catalytic nucleic acids has enabled them to act as reporter molecules for biosensing applications, and several such biosensors have been reported for the analysis of different metal ions.[12] To explore the new dimensions of this interesting research area, we developed a system of logic gates (OR, AND, and INHIBIT) based entirely on colorimetric outputs. The system is obtained by using a series of supramolecular circular structures with different repeat units based on ion-dependent DNAzymes, in which the DNAzyme cofactors, that is Pb^{2+} and Mg^{2+} ions, are used as inputs for the activation of the respective scission DNAzymes. Upon cleavage, the substrates yield overhung segments for the attachment of single DNA–AuNP probes as output. The colorimetric signals can be read out in the presence of the appropriate inputs. In addition, based on the principles of DNA hybridization and strand displacement,[13] an XOR logic gate operation is achieved. Moreover, by employing binary DNA–AuNP probes as colorimetric signal output, a NOR gate was designed, and XNOR and NAND gates are demonstrated on the basis of XOR and AND gates, respectively. To the best of our knowledge, the application of colorimetric detection for logic gate operations based on DNAzyme-catalyzed DNA cleavage has not been reported to date.

Figure 1 shows the construction of the OR gate. The Mg^{2+}-dependent DNAzyme **1** and the Pb^{2+}-dependent DNAzyme **2** hybridize with the circular substrate **3**. The OR gate consists of a supramolecular structure **I**, and single $DNA_{a\text{-}b}$–AuNP probes that are complementary to the sequence of A–B in **I**. The circular substrate **3** with four repeated A–B sequence units (B-A/rA/A-B/B-A/rA/A-B) includes two ribonucleobases (rAs) as cleavable sites for Mg^{2+}- and Pb^{2+}-dependent DNAzymes, respectively.

In order to avoid the cross-reactions of DNAzymes that result from the repeat units of the circular substrate, additional sequences are designed for the respective rAs (black strands for Mg^{2+}-dependent DNAzymes; light blue strands for Pb^{2+}-dependent DNAzymes in Figure 1), which should ensure that Mg^{2+}- and Pb^{2+}-dependent DNAzymes recognize specific regions of the circular substrate and form the

[*] Dr. S. Bi, Y. Yan, S. Hao, Prof. Dr. S. Zhang
Key Laboratory of Eco-chemical Engineering, Ministry of Education
College of Chemistry and Molecular Engineering
Qingdao University of Science and Technology
Qingdao 266042 (P.R. China)
Fax: (+86)-532-8402-2750
E-mail: shushzhang@126.com

[**] This work was supported by the Excellent Young Scientists Foundation of Shandong Province (JQ200805), the University Doctoral Foundation of the Ministry of Education (200804260001), and the National Basic Research Program of China (2010CB732404).

Supporting information for this article is available on the WWW under http://dx.doi.org/10.1002/anie.201000840.

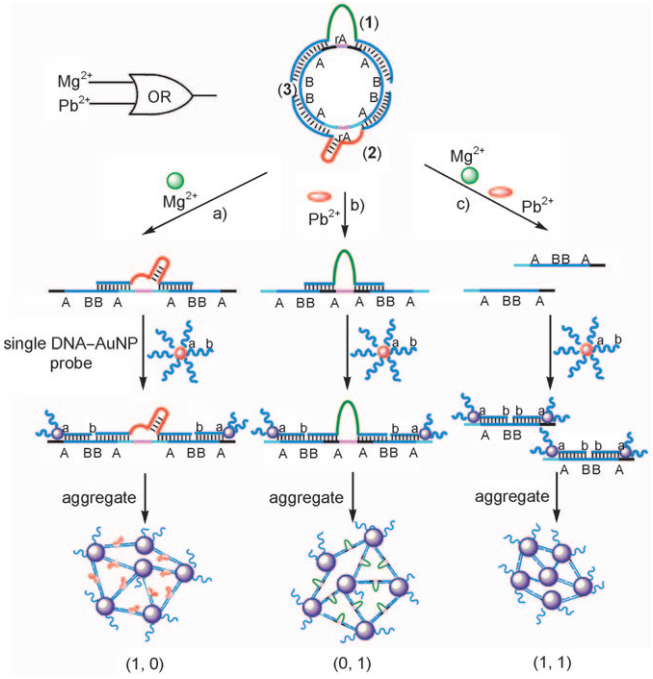

Figure 1. OR logic gate system that is activated by Mg^{2+} and Pb^{2+} ions as inputs and connected to single $DNA_{a\text{-}b}$–AuNP probes as colorimetric outputs. Circuits are operated as described in the main text. AuNPs are represented by red spheres and AuNP aggregates are represented by purple spheres.

anticipated supramolecular structure of the OR and other logic gates. The additional specific recognition sequences are designed as substrate strands for Mg^{2+}- and Pb^{2+}-dependent DNAzymes, respectively.[6,7] In addition, the construction of the supramolecular structure **I**, which is obtained by hybridizing **3** with the arms of the two DNAzymes, prohibits it from being hybridized with single $DNA_{a\text{-}b}$–AuNP probes before the gate is triggered. That is, in the absence of Mg^{2+} and Pb^{2+} ions, the color of the DNA–AuNPs solution is red (output 0). However, in the presence of either Mg^{2+} ions (pathway a) or Pb^{2+} ions (pathway b), the reaction of the supramolecular complex with either input results in the cleavage of the substrate **3** at the respective rA. Either of the scission processes yields a nucleic acid fragment including the A-B/B-A/rA/A-B/B-A output strand. Thus, single $DNA_{a\text{-}b}$–AuNP probes are hybridized with the two overhangs of the fragment, and result in the aggregation of AuNPs that leads to the characteristic color change from red to purple (output 1), which characterizes the OR logic gate. When both inputs are present (pathway c), the two rAs in the circular substrate **3** are cleaved simultaneously, which results in the instability of the duplex structure between the two ion-dependent DNAzymes and the fragments of the substrate. The circular substrate **3** separates into the output A-B/B-A strands since it possesses two A-B/B-A units when the two rAs are cleaved simultaneously. Thus, a color change of AuNPs is obtained when the system is subjected to one ion input, Mg^{2+} (1,0), Pb^{2+} (0,1) or two ion inputs (1,1). In addition, the gel electrophoresis images obtained upon Mg^{2+}- or Pb^{2+}-induced cleavage of substrate **3** by the ion-dependent DNAzymes **1** and **2** confirm that the stability of the duplexes of the DNAzyme units hybridized with the circle domains is very similar before and after cleavage by the DNAzyme (Figure S2 in the Supporting Information).

After optimizing the amount of single $DNA_{a\text{-}b}$–AuNP probes used in OR logic gates (see the Supporting Information for details), Figure 2 shows the results of colorimetric

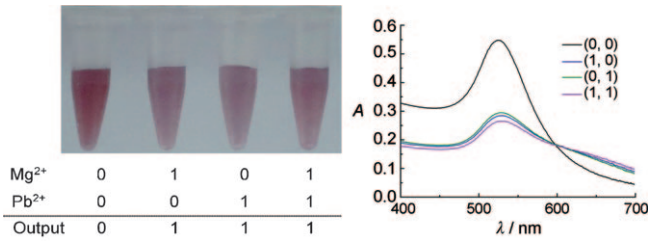

Figure 2. The results of each path of the OR gate are characterized by colorimetric and UV/Vis detection. The average diameter of AuNPs is ca. 42 nm.

experiments carried out by activating **I**. We also investigated the system by using UV/Vis spectroscopy. While the absorption maximum is located at 526 nm in the absence of any ion input (0,0), the activation of the system with either Mg^{2+} or Pb^{2+} ions leads to a shift of the peak to approximately 530 nm, which results from the aggregation of AuNPs. Also, when the system is subjected to both inputs, the purple curve, which is a "true" output, is obtained (the truth table is shown in Figure 2).

In addition, because OR logic is represented by the situation where the output of an OR gate is true if either inputs is true, we employed the OR logic gate to perform control experiments in order to demonstrate the selectivities of the system. The logic gates demonstrate good selectivities for Mg^{2+} and Pb^{2+} ion inputs compared with other divalent metal ions (see Figure S4 in the Supporting Information). Together, these results validate the use of supramolecular structures of specific ion-dependent DNAzymes for the fabrication of metal-ion colorimetric logic gates. Moreover, the activity of DNAzymes and cross-talk between Mg^{2+} and Pb^{2+} ions have also been investigated (see the Supporting Information).

The ion-dependent DNAzyme sequences **4** and **5** were used to construct the AND gate. The AND logic is represented by the situation where the output of an AND gate is true only if both inputs are true. Figure 3a shows the functional principle of the AND gate construction. The two DNAzyme sequences **4** and **5** are hybridized with the circular substrate **6**, resulting in a supramolecular structure **II**. The circular substrate **6** consists of the specific sequence (D-C/rA/A-B/B-A/rA/C-D) including two rAs as cleavable sites for each of the DNAzymes. In the presence of either Mg^{2+} or Pb^{2+} ions, only one rA specific to Mg^{2+} or Pb^{2+} ions is cleaved and the structure of substrate **6** is opened from circular to strand form (A-B/B-A/rA/C-D/D-C), with a duplex structure in the middle region. In this case, single $DNA_{a\text{-}b}$–AuNP probes can only hybridize with one end of the opened circular substrate

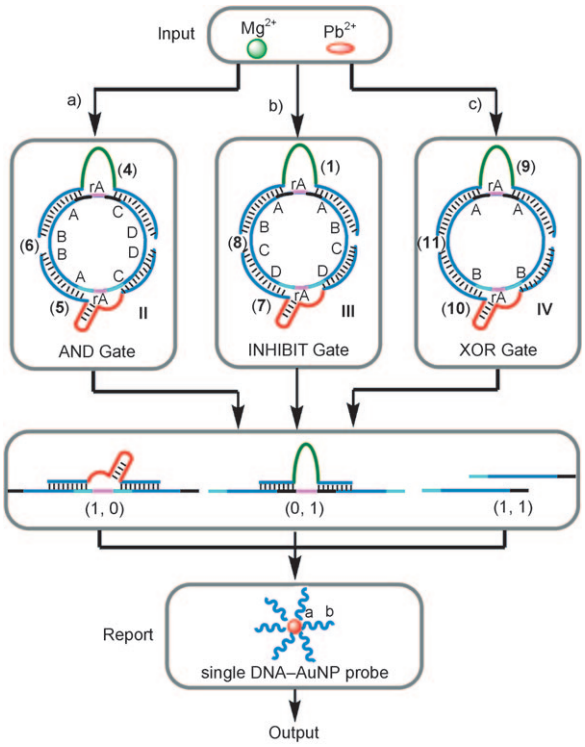

Figure 3. AND, INHIBIT, and XOR logic gates connected to single $DNA_{a\text{-}b}$–AuNP probes as colorimetric outputs. Each path is characterized by colorimetric and UV/Vis detection. The detailed schematic illustrations and results are given in the Supporting Information.

(A-B); this hybridization leads to a red solution and thus the output 0. In turn, treatment of structure **II** with both Pb^{2+} and Mg^{2+} ions, results in the cleavage of substrate **6** at the two rAs into two DNA strands (A-B/B-A and C-D/D-C). Thus, the single $DNA_{a\text{-}b}$–AuNPs can be assembled on the A-B/B-A strand in a "tail-to-tail" manner to form purple aggregates, which are considered as output 1 (see Figure S5 in the Supporting Information for the colorimetric and UV/Vis results). In addition, these phenomena are consistent with the assumption that the aggregates of AuNPs in this study are actually assembled by the DNA linkers, and leads to a red shift in the surface plasmon resonance (see AND gate in Supporting Information). It is noteworthy that because DNA hybridization at AuNP surfaces does not significantly affect the optical properties and cannot account for the surface plasmon band changes associated with AuNP aggregation.[14] Thus, there is no significant surface plasmon band changes observed for the outputs of (1,0) and (0,1) compared to that of (0,0).

An INHIBIT gate, which consisted of two DNAzymes **1** and **7**, and a circular substrate **8** (B-A/rA/A-B/C-D/rA/D-C) was also designed (Figure 3b). When only Mg^{2+} ions were added, the output was 1, otherwise it was 0 (Figure S6 in the Supporting Information). These results indicate that Mg^{2+} and Pb^{2+} DNAzymes really function as a two-input INHIBIT logic gate (see Figure S 6 in the Supporting Information for the truth table).

As described above, the circular substrate, which is the core component of the three logic gates (OR, AND, and INHIBIT), can be divided into four units, such as four A–B units for the OR gate, and two A–B units and two C–D units for AND and INHIBIT gates. A smaller circular substrate **11**, which also contained two rAs but only two A–B regions (A-B/rA/B-A/rA) was designed to achieve an XOR gate operation based on the principles of DNA hybridization and strand displacement (Figure 3c).[13] Unlike the other gates, in which each arm of the DNAzyme is hybridized completely with one unit of circular substrate, each arm is only hybridized with half of the A-B unit in the XOR gate. Thus, in the presence of either Mg^{2+} or Pb^{2+} ions, only half of the A–B sequence at the two ends of the substrate is overhung. However, upon addition of single $DNA_{a\text{-}b}$–AuNP probes, the full-length complementary $DNA_{a\text{-}b}$ strand (12-mer) at the AuNP surface is hybridized with the overhung segment (half A-B sequence, 6-mer), which is known as a "toehold" and proceeds to invade and displace the previously hybridized sequences by a principle termed "toehold exchange" (the detailed steps are illustrated in Figure 4).[13a]

This phenomenon eventually results in the assembly of AuNPs at both ends of the cleaved substrate, and gives rise to the output of 1, although the displacement reaction may not proceed to completion, which can be attributed to a limited number of bases in the $DNA_{a\text{-}b}$ strand. Interestingly, in this logic operation, the purple aggregates are formed by aligning the nanoparticles in a "tail-to-tail" manner (pathway a in Figure 4) and a "head-to-head" manner (pathway b in Figure 4), respectively. However, when both inputs are present, the circular substrate is cleaved into two single strands that contain only one A–B region. As described above, there is no significant difference between the UV/Vis spectra of the single- and double-DNA-modified AuNPs. Thus, after the single $DNA_{a\text{-}b}$-AuNP probes are hybridized with the cleaved single-stranded DNA, no color- and surface plasmon band change is observed, and the output is 0 (see Figure S7 in the Supporting Information).

For the above logic gate operations, all the outputs of the ground state (0,0) are false (0). However, in electronic Boolean logic gates, it is also necessary to achieve a true value of the (0,0) state to meet the requirements of other logic gate operations. Inspired by the above DNA hybridization and displacement mechanism, a binary DNA–AuNP probe was

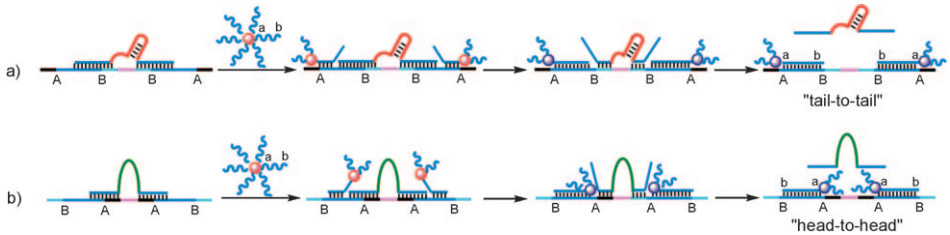

Figure 4. Representation of the DNA displacement principle applied in the XOR logic gate.

designed to create a NOR logic gate. Briefly, a linker DNA (12-mer) is designed to have two "sticky ends" (6-mer) that are complementary to the tail sequence of $DNA_{a\text{-}b}$ in a single $DNA_{a\text{-}b}$–AuNP probe, thus resulting in a tail-to-tail binary $DNA_{a\text{-}b}$–AuNP probe. In this case, the aggregates of AuNPs are formed and the output of 1 for the ground state (0,0) is obtained.

In the NOR logic operation (Figure 5), a circular substrate **13** containing two rAs and four alternant units (D-C/rA/A-B/D-C/rA/A-B) is hybridized with two DNAzyme sequences **4**

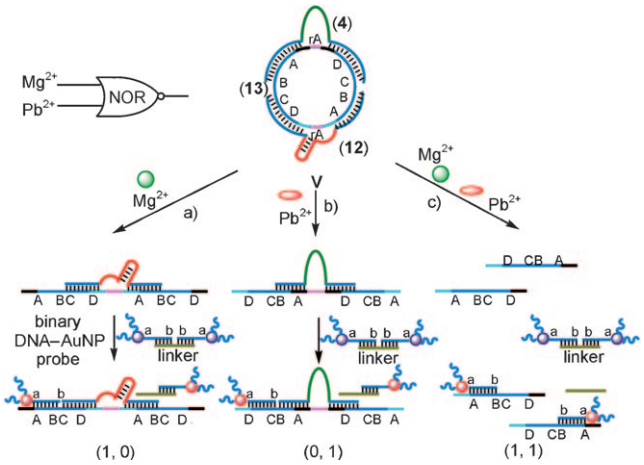

Figure 5. NOR logic gate system connected to binary $DNA_{a\text{-}b}$–AuNP probes as colorimetric outputs. Circuits are operated as described in the main text.

and **12** to construct the supramolecular structure **V**. In the presence of either Mg^{2+} or Pb^{2+} ions, the circular substrate is cleaved by the ion-dependent DNAzyme at the respective rA cleavage site. Since the stability of the 12-mer-long duplex is greater than that of a 6-mer-long duplex, $DNA_{a\text{-}b}$–AuNPs are more favorably hybridized with the 12-mer A-B unit sequence overhung at one end of the cleaved substrate that is complementary to the $DNA_{a\text{-}b}$ sequence. This process results in the dissociation of binary $DNA_{a\text{-}b}$–AuNP probes from a 6-mer duplex region. The feasibility of this process has been proved by kinetic studies.[13c,15] In principle, this displacement process should result in a dark-red solution, which is nearly identical to that of single $DNA_{a\text{-}b}$–AuNP probes. However, only a reddish color could be observed for pathway a and b, respectively, while the intensities of the plasmon band are apparently increased (see Figure S8 in the Supporting Information). Similarly, in the presence of both Mg^{2+} and Pb^{2+} ions, the circular substrate is cleaved into two strands containing only one A–B unit, which could also displace the $DNA_{a\text{-}b}$ sequence of the binary DNA–AuNP probes, hence resulting in an output of 0. In this case, if observed carefully, the red color of pathway c is slightly darker than that of pathway a or pathway b, which can be attributed to the double amount of A–B units yielded in pathway c. The results are consistent with those obtained by UV/Vis detection (Figure S8 in the Supporting Information).

To demonstrate the flexibility of the logic gates, we used the constructed XOR gate and AND gate as platforms to design a NAND gate and a XNOR gate, respectively, by employing binary $DNA_{a\text{-}b}$–AuNP probes as colorimetric output (Figure 6). In electronics, NAND logic is the result

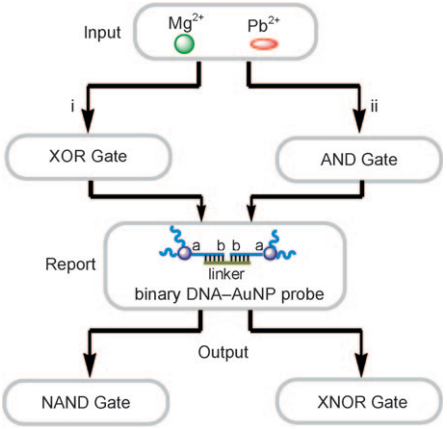

Figure 6. Representation of NAND and XNOR logic gates connected to binary $DNA_{a\text{-}b}$–AuNP probes as colorimetric outputs. Each path is characterized by colorimetric and UV/Vis detection. The detailed schematic illustrations and results are given in the Supporting Information.

of sending an AND gate through an inverter, which causes all 0 states to switch to 1 and vice versa, while XNOR logic is the inverted result of an XOR gate. Thus, NAND logic has an output of 1 for the inputs (0,0), (1,0), and (0,1). For the (1,1) situation, the output now becomes 0 (Figure S9). XNOR logic has an output 1 for (0,0) and (1,1), and 0 for (1,0) and (0,1) (Figure S10 in the Supporting Information).

In order to demonstrate the performance of these novel functions through rational gate networking, we connected the AND and XOR gates into a multilevel circuit that enforced an overall OR Boolean behavior (Figure 7; see Figure S11 in the Supporting Information for colorimetric and UV/Vis results).

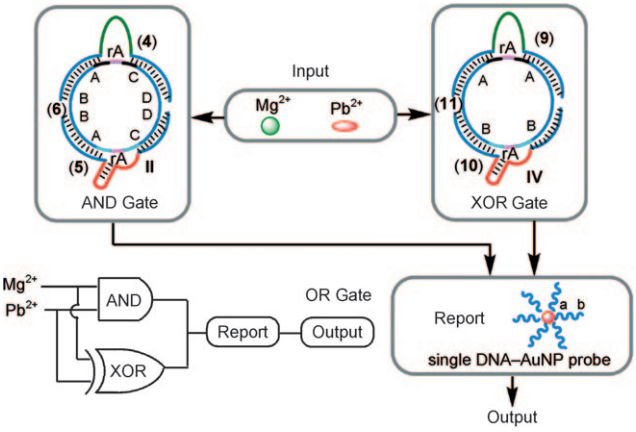

Figure 7. Multilevel circuit built from an AND and a XOR gate performs an overall OR analysis on the inputs. The function of the circuit was assayed using the single $DNA_{a\text{-}b}$ probes as reporters.

In conclusion, by designing a series of circular substrates, we have constructed a complete set of two-input logic gates (OR, AND, INHIBIT, XOR, NOR, NAND, and XNOR) based on the use of ion-dependent DNAzymes as functional components and the respective cofactor-ions as inputs. The outputs of the cleaved active sites of the gates perform the gate functions by AuNP-based homogeneous colorimetric detection. This simple and complete gate design could become a general method for any metal ion of interest with a specific DNAzyme and other targets, such as theophylline and cyclic guanosine monophosphate (cGMP) based on aptazymes. In the future, this logic system can be developed into portable test kits or strips, which allows fast metal-ion detection at ambient temperature and therefore shows great promise for practical onsite applications.

Received: February 10, 2010
Revised: March 19, 2010
Published online: May 7, 2010

Keywords: aggregation · DNA structures · logic gates · molecular devices · nanoparticles

[1] J. P. Hayes, *Introduction To Digital Logic Design*, Addison-Wesley Publishing Company, Reading, MA, **1993**.
[2] a) M. Ogihara, A. Ray, *Nature* **2000**, *403*, 143 – 144; b) Y. Benenson, T. Paz-Elizur, R. Adar, E. Keinan, Z. Livneh, E. Shapiro, *Nature* **2001**, *414*, 430 – 434; c) J. H. Reif, *Science* **2002**, *296*, 478 – 479; d) Y. Benenson, B. Gil, U. Ben-Dor, R. Adar, E. Shapiro, *Nature* **2004**, *429*, 423 – 429; e) A. P. De Silva, *Nat. Mater.* **2005**, *4*, 15 – 16.
[3] a) C. Mao, T. H. LaBean, J. H. Reif, N. C. Seeman, *Nature* **2000**, *407*, 493 – 496; b) G. Seelig, D. Soloveichik, D. Y. Zhang, E. Winfree, *Science* **2006**, *314*, 1585 – 1588; c) J. Elbaz, M. Moshe, I. Willner, *Angew. Chem.* **2009**, *121*, 3892 – 3895; *Angew. Chem. Int. Ed.* **2009**, *48*, 3834 – 3837; d) X. Feng, X. Duan, L. Liu, F. Feng, S. Wang, Y. Li, D. Zhu, *Angew. Chem.* **2009**, *121*, 5420 – 5425; *Angew. Chem. Int. Ed.* **2009**, *48*, 5316 – 5321; e) B. M. Frezza, S. L. Cockroft, M. R. Ghadiri, *J. Am. Chem. Soc.* **2007**, *129*, 14875 – 14879; f) D. Miyoshi, M. Inoue, N. Sugimoto, *Angew. Chem.* **2006**, *118*, 7880 – 7883; *Angew. Chem. Int. Ed.* **2006**, *45*, 7716 – 7719.
[4] a) W. Xu, X. Xue, T. Li, J. Zeng, X. Liu, *Angew. Chem.* **2009**, *121*, 6981 – 6984; *Angew. Chem. Int. Ed.* **2009**, *48*, 6849 – 6852; b) M. K. Beissenhirtz, R. Elnathan, Y. Weizmann, I. Willner, *Small* **2007**, *3*, 375 – 379.
[5] H. L. Needleman, *Human Lead Exposure*, CRC, Boca Raton, FL, **1992**.
[6] E. Rubenowitz, G. Axelsson, R. Rylander, *Am. J. Epidemiol.* **1996**, *143*, 456 – 462.
[7] R. R. Breaker, *Science* **2000**, *290*, 2095 – 2096.
[8] J. Liu, Y. Lu, *J. Am. Chem. Soc.* **2003**, *125*, 6642 – 6643.
[9] J. Elbaz, M. Moshe, B. Shlyahovsky, I. Willner, *Chem. Eur. J.* **2009**, *15*, 3411 – 3418.
[10] M. Moshe, J. Elbaz, I. Willner, *Nano Lett.* **2009**, *9*, 1196 – 1200.
[11] J. Liu, Y. Lu, *J. Am. Chem. Soc.* **2007**, *129*, 9838 – 9839.
[12] a) J. Liu, Z. Cao, Y. Lu, *Chem. Rev.* **2009**, *109*, 1948 – 1998; b) I. Willner, B. Shlyahovsky, M. Zayats, B. Willner, *Chem. Soc. Rev.* **2008**, *37*, 1153 – 1165; c) J. Liu, Y. Lu, *J. Am. Chem. Soc.* **2005**, *127*, 12677 – 12683.
[13] a) D. Y. Zhang, A. J. Turberfield, B. Yurke, E. Winfree, *Science* **2007**, *318*, 1121 – 1125; b) P. Yin, H. M. T. Choi, C. R. Calvert, N. A. Pierce, *Nature* **2008**, *451*, 318 – 322; c) Z. Zhang, Q. Cheng, P. Feng, *Angew. Chem.* **2009**, *121*, 124 – 128; *Angew. Chem. Int. Ed.* **2009**, *48*, 118 – 122.
[14] J. J. Storhoff, A. A. Lazarides, R. C. Mucic, C. A. Mirkin, R. L. Letsinger, G. C. Schatz, *J. Am. Chem. Soc.* **2000**, *122*, 4640 – 4650.
[15] a) P. Hazarika, B. Ceyhan, C. M. Niemeyer, *Angew. Chem.* **2004**, *116*, 6631 – 6633; *Angew. Chem. Int. Ed.* **2004**, *43*, 6469 – 6471; b) L. P. Reynaldo, A. V. Vologodskii, B. P. Neri, V. I. Lyamichev, *J. Mol. Biol.* **2000**, *297*, 511 – 520; c) C. K. Tison, V. T. Milam, *Langumir* **2007**, *23*, 9728 – 9736.

